Turkish J. Eng. Env. Sci.
29 (2005) , 51 – 60.

Yielding and Elastoplastic Deformation of Annular Disks of a Parabolic Section Subject to External Compression

Ahmet N. ERASLAN, Ferhat AKGÜL
Middle East Technical University, Department of Engineering Sciences
Ankara-TURKEY
e-mail: aeraslan@metu.edu.tr

Received 03.09.2004

Abstract

A computational model is developed to predict partially plastic stresses in variable thickness annular disks subject to radial compression. The model is based on the von Mises' yield criterion, deformation theory of plasticity and a Swift type hardening law. Considering a thickness profile in the form of a general parabolic function, the condition of occurrence of plastic deformation at the inner and outer edges of the annular disk is investigated. A critical disk profile is determined and the corresponding elastic-plastic stress as well as the residual stress distribution is computed.

Key words: Variable thickness, External pressure, Nonlinear hardening, Residual stresses, von Mises criterion.

Introduction

For the design of rotating or nonrotating disks in many industrial applications, in order to achieve efficiency in design, the stresses in these objects under different boundary conditions must be examined. Such a need has generated much research in this field. The subject of stationary disks under external pressure was first studied by Gamer (1984a, 1984b). In his investigations, Gamer considered a uniform thickness annular disk and obtained analytical solutions of the elastic-plastic deformation caused by the application of pressure at the edge of the disk for linear strain hardening. The analytical solution presented by Gamer was based on Tresca's yield criterion and its associated flow rule. It was shown that the plastic region in the uniform thickness annular disk first forms at the inner surface and propagates outwards with increasing pressures. Güven (1992) extended Gamer's work using the same basic assumptions to an annular disk of variable thickness in hyperbolic form. In his later work, Güven (1993) considered an annular disk profile in exponential form and studied the effect of the application of external pressure analytically. In both of these studies (Güven, 1992; 1993), it was assumed that the plastic deformation commenced at the inner surface of the disk. A numerical solution of the problem for an annular disk of nonlinearly hardening material behavior exhibiting linearly tapered thickness was presented by You and Zhang (1998). Their analysis was based on von Mises' yield criterion and deformation theory of plasticity. They reported that for small aspect ratios different types of plastic deformation might occur. Recently, Güven (1998) introduced 2 thickness functions, one in power function form, and the other in parabolic form both involving 2 geometric parameters to describe the variation of the thickness of annular disks. Analytical solutions for disks having such profiles were obtained with free and pressurized boundary conditions. Similar thickness profiles were then used by Eraslan and Apatay (2004) to investigate different modes of plastic deformation for small aspect ratios. Considering the stresses in a purely elastic state it was shown that there exists a critical thickness profile for which plastic flow takes

place at the inner and outer surfaces of the annular disk simultaneously under compression. However, this work was limited to elastic deformations and partially plastic behaviour was not studied.

In this paper, the relationship between the geometry of variable thickness annular disks and the radial locations of the formation and development of plastic regions under external pressure are investigated. A unified treatment of the boundary value problem under consideration is presented using the von Mises yield criterion, the deformation theory of plasticity and a general nonlinear strain hardening material behavior. A critical disk profile for which yielding commences at both annular surfaces simultaneously is determined and stress analysis results are presented for the partially plastic and fully plastic stress states for this profile. The residual stresses occurring in such disks upon complete unloading of external pressure are also determined.

The Parabolic Disk

In this work, we consider a thin annular disk whose thickness varies continuously in the form of a general parabolic function $h(r)$ (Eraslan, 2003)

$$h(r) = h_0 \left[1 - \left(\frac{r}{b+n}\right)^k\right], \tag{1}$$

where h_0, n and k are parameters ($h_0 > 0$, $n > 0$, $k \geq 0$), and b is the outer radius of the annular disk. With this form of the profile function, a uniform thickness disk is obtained by setting $n \to \infty$ and a linearly decreasing disk thickness is obtained by the use of $k = 1$. If $k < 1$ the profile is concave and if $k > 1$ it is convex. Furthermore, the shape of the profile is smoothed as n increases. It should be noted that the elastoplastic model developed herein is not limited to this thickness variation. It can be used for variable thickness with any functional form of thickness variability.

Basic Equations and Elastic Solution

A state of plane stress ($\sigma_z = 0$) and small deformations are presumed. The thickness of the disk is assumed to be sufficiently small compared to its diameter so that plane stress assumption is justified (Timoshenko and Goodier, 1970). The strain-displacement relations for small strains $\epsilon_r = du/dr$ and $\epsilon_\theta = u/r$, the equation of equilibrium in radial direction

$$\frac{d}{dr}(hr\sigma_r) - h\sigma_\theta = 0, \tag{2}$$

the compatibility

$$\frac{d}{dr}(r\epsilon_\theta) - \epsilon_r = 0, \tag{3}$$

and generalized Hooke's law

$$\epsilon_r = \epsilon_r^e + \epsilon_r^p = \frac{1}{E}\left[\sigma_r - \nu\sigma_\theta\right] + \epsilon_r^p, \tag{4}$$

$$\epsilon_\theta = \epsilon_\theta^e + \epsilon_\theta^p = \frac{1}{E}\left[\sigma_\theta - \nu\sigma_r\right] + \epsilon_\theta^p, \tag{5}$$

$$\gamma_{r\theta} = 0, \tag{6}$$

hold in the entire annular disk irrespective of the material behavior. In the equations above σ_r and σ_θ denote the radial and circumferential stress components, E the modulus of elasticity, ϵ_r and ϵ_θ the radial and circumferential strain components, ν the Poisson's ratio and $\gamma_{r\theta}$ the shearing strain. The superscripts e and p stand for elastic and plastic counterparts of total strains ϵ_r and ϵ_θ. In purely elastic deformations $\epsilon_j^p = 0$, and a straightforward manipulation on strain-displacement relations and Hooke's law results in the following stress-displacement relations:

$$\sigma_r = \frac{E}{1-\nu^2}\left[\frac{\nu u}{r} + u'\right], \tag{7}$$

$$\sigma_\theta = \frac{E}{1-\nu^2}\left[\frac{u}{r} + \nu u'\right], \tag{8}$$

in which a prime denotes differentiation with respect to the radial coordinate r. Substitution of the disk thickness profile from Eq. (1), the stresses from Eqs. (7) and (8) in the equation of equilibrium (2), leads to the following homogeneous differential equation in radial displacement u:

$$r^2\left[1 - \left(\frac{r}{b+n}\right)^k\right]\frac{d^2u}{dr^2} + r\left[1 - (1+k)\left(\frac{r}{b+n}\right)^k\right]\frac{du}{dr} - \left[1 - (1-k\nu)\left(\frac{r}{b+n}\right)^k\right]u = 0. \tag{9}$$

The exact solution is achieved by using a new variable $z = [r/(b+n)]^k$ and the transformation $u(r) =$

$ry(z)$. After some algebraic manipulations, Eq. (9) is transformed into

$$z(1-z)\frac{d^2y}{dz^2}+\frac{1}{k}[2+k-2(1+k)z]\frac{dy}{dz}-\frac{1}{k}(1+\nu)\,y=0. \tag{10}$$

This is the standard form of the hypergeometric differential equation with the solution (Abramowitz and Stegun, 1966)

$$y(z)=C_1F(\alpha,\beta,\delta;z)+\hat{C}_2\,z^{-\frac{2}{k}}F(\alpha-\delta+1,\ \beta-\delta+1,2-\delta;z) \tag{11}$$

where C_i is an arbitrary integration constant and $F(\alpha,\beta,\delta;z)$ is the hypergeometric function defined by

$$F(\alpha,\beta,\delta;z)=1+\frac{\alpha\beta}{\delta 1!}z+\frac{\alpha(\alpha+1)\beta(\beta+1)}{\delta(\delta+1)2!}z^2 +\frac{\alpha(\alpha+1)(\alpha+2)\beta(\beta+1)(\beta+2)}{\delta(\delta+1)(\delta+2)3!}z^3+\cdots. \tag{12}$$

The arguments α, β and δ of the hypergeometric function F in Eq. (11) have the following meanings:

$$\alpha=\frac{1}{2}+\frac{1}{k}-\frac{\sqrt{k^2+4(1-k\nu)}}{2k}, \tag{13}$$

$$\beta=\frac{1}{2}+\frac{1}{k}+\frac{\sqrt{k^2+4(1-k\nu)}}{2k}, \tag{14}$$

$$\delta=1+\frac{2}{k}. \tag{15}$$

The general solution for the radial displacement can now be expressed as

$$u(r)=C_1P(r)+C_2Q(r), \tag{16}$$

where

$$P(r)=rF\left(\alpha,\beta,\delta;\left(\frac{r}{b+n}\right)^k\right), \tag{17}$$

$$Q(r)=\frac{1}{r}F\left(\alpha\delta+1,\beta-\delta+1,2-\delta;\left(\frac{r}{b+n}\right)^k\right). \tag{18}$$

Substituting the displacement solution (16) in stress-displacement relations (7) and (8) one obtains

$$\sigma_r=\frac{E}{1-\nu^2}\left[C_1\left(\frac{\nu P}{r}+P'\right)+C_2\left(\frac{\nu Q}{r}+Q'\right)\right], \tag{19}$$

$$\sigma_\theta=\frac{E}{1-\nu^2}\left[C_1\left(\frac{P}{r}+\nu P'\right)+C_2\left(\frac{Q}{r}+\nu Q'\right)\right]. \tag{20}$$

The derivatives P' and Q' in Eqs. (19) and (20) are evaluated using the differentiation rule (Abramowitz and Stegun, 1966)

$$\frac{d}{dr}F\left(\alpha,\beta,\delta;z(r)\right)=\frac{\alpha\beta}{\delta}\frac{dz}{dr}F\left(\alpha+1,\beta+1,\delta+1;z(r)\right). \tag{21}$$

The elastic solution is completed by the application of the boundary conditions. For an annular disk with bore radius a, subject to external pressure p, boundary conditions read $\sigma_r(a)=0$ and $\sigma_r(b)=-p$. Accordingly, the integration constants are evaluated as

$$C_1=\frac{-bp(1-\nu^2)[\nu Q(a)+aQ'(a)]}{D},\qquad C_2=\frac{-bp(1-\nu^2)[\nu P(a)+aP'(a)]}{D}, \tag{22}$$

in which

$$D=E\{[\nu Q(a)+aQ'(a)][\nu P(b)+bP'(b)]-[\nu Q(b)+bQ'(b)][\nu P(a)+aP'(a)]\}. \tag{23}$$

On the other hand, for plane stress, the von Mises yield criterion takes the form (Mendelson, 1968)

$$\sigma_Y=\sqrt{\sigma_r^2-\sigma_r\sigma_\theta+\sigma_\theta^2}. \tag{24}$$

The disk will yield, that is, the plastic deformation in the disk will begin as soon as $\sigma_Y\geq\sigma_0$ with σ_0 being the uniaxial yield limit of disk material. Elastic limit pressure $p_e=p_1$ is calculated from $\sigma_Y=\sigma_0$.

For small aspect ratios ($\overline{a}=a/b$) different forms of plastic flow may occur. Figure 1 depicts the set of k vs. n values for which the plastic deformation commences simultaneously at both the inner and outer surfaces of the annular disk for aspect ratios $\overline{a}=0.1$, 0.2, 0.3 and 0.4. If the geometric parameters are located on the left of the curves, plastic flow begins first at the outer surface and otherwise at the inner surface. We consider the aspect ratio $\overline{a}=0.2$. For the parameter $n=0.4$, the critical value of k for which yielding sets in simultaneously

at both surfaces is determined as 1.02467 (see Figure 1). This critical disk profile is drawn in Figure 2. Note that the profile is almost linear with outer edge thickness $h(b) = 0.292 \cdot h_0$. The elastic limit pressure for this critical profile is determined as $\overline{p}_1 = p_1/\sigma_0 = 1.10720$. Figure 3 shows the corresponding nondimensional stresses, $\overline{\sigma}_j = \sigma_j/\sigma_0$ and nondimensional displacement $\overline{u} = uE/\sigma_0 b$ in the annular disk. The stress variable ϕ in this figure is obtained from

$$\phi = \sqrt{\overline{\sigma}_r^2 - \overline{\sigma}_r\overline{\sigma}_\theta + \overline{\sigma}_\theta^2}. \tag{25}$$

Note that according to the von Mises yield criterion (24), $\phi = 1$ states an elastic-plastic border. As seen in Figure 3, $\phi(a) = \phi(b) = 1$, indicating the initiation of plastic flow at both surfaces simultaneously.

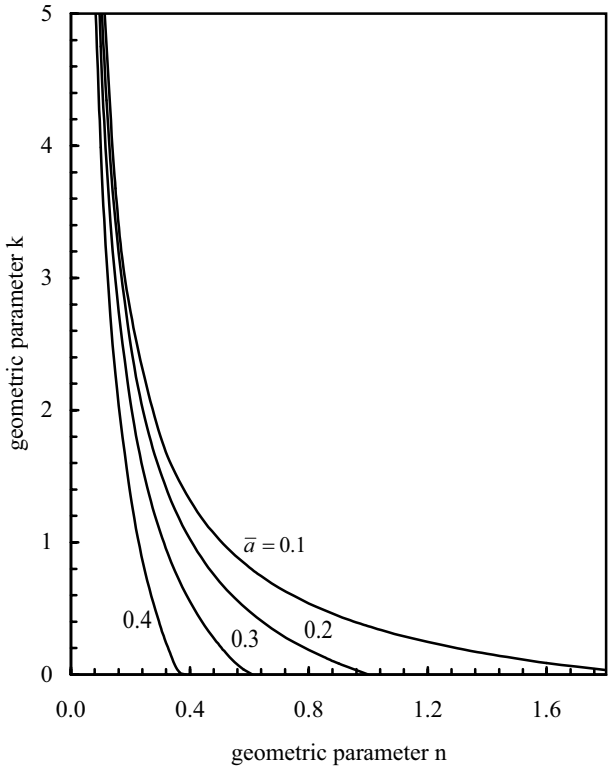

Figure 1. Critical disk profile parameters for which yielding sets in simultaneously at the inner and outer surface for different values of $\overline{a} = a/b$.

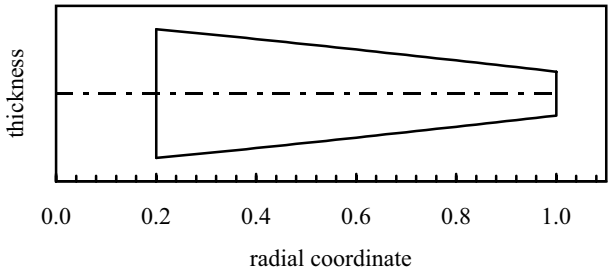

Figure 2. Critical disk profile for $\overline{a} = 0.2$ ($n = 0.4$, $k = 1.02467$).

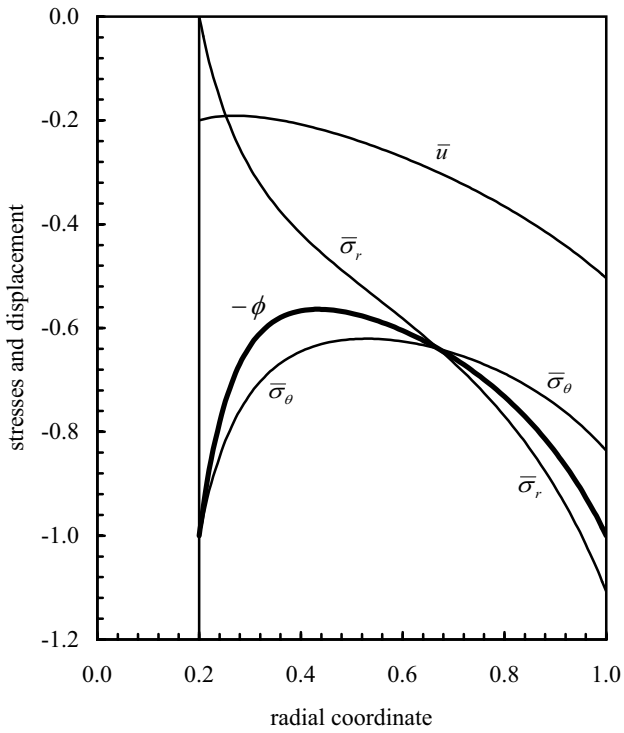

Figure 3. Elastic stresses and displacement in the critical disk profile for $\overline{a} = 0.2$, ($n = 0.4$, $k = 1.02467$ and $\overline{p}_1 = 1.10720$).

Elastic-Plastic Solution

As stated earlier, the computational model developed in this section is valid for variable thickness with any functional form of thickness variability. Defining the stress function in terms of radial stress

$$Y(r) = rh\sigma_r, \tag{26}$$

and using the equation of motion (2) one obtains

$$\sigma_r = \frac{Y}{hr} \quad \text{and} \quad \sigma_\theta = \frac{1}{h}\frac{dY}{dr}. \tag{27}$$

Expressing the elastic strains ϵ_r^e and ϵ_θ^e in terms of the stress function $Y(r)$ and substituting them in the compatibility relation (3) leads to the following governing differential equation for elastic behavior:

$$\frac{d^2Y_e}{dr^2} + \left[\frac{1}{r} - \frac{h'}{h}\right]\frac{dY_e}{dr} - \left[\frac{1}{r^2} - \frac{\nu h'}{rh}\right]Y_e = 0, \quad (28)$$

where Y_e denotes the stress function in the elastic region. Similarly, if the total strains from Eqs. (4) and (5) are substituted in the compatibility relation (3) and making use of Eq. (27) one obtains the governing differential equation for the plastic region

$$\frac{d^2Y_p}{dr^2} + \left[\frac{1}{r} - \frac{h'}{h}\right]\frac{dY_p}{dr} - \left[\frac{1}{r^2} - \frac{\nu h'}{rh}\right]Y_p = -\frac{Eh}{r}\left[\epsilon_\theta^p + r\frac{d\epsilon_\theta^p}{dr} - \epsilon_r^p\right], \quad (29)$$

in which Y_p denotes the stress function in the plastic region. Note that at the elastic-plastic border r_{ep}, for the stresses σ_r and σ_θ to be continuous, from Eq. (27) it is required that the stress function and its first derivative must be continuous, that is $Y_e(r_{ep}) = Y_p(r_{ep})$ and $Y_e'(r_{ep}) = Y_p'(r_{ep})$. Since the plastic strains and their first derivatives on the right hand side of Eq. (29) are not known a priori, further elaboration is necessary. This is done next.

According to Henky's deformation theory, the plastic strains ϵ_r^p, ϵ_θ^p, and ϵ_z^p are given as (Mendelson, 1968; Chen and Han, 1988)

$$\epsilon_r^p = \frac{\epsilon_{EQ}}{\sigma_Y}\left[\sigma_r - \frac{1}{2}\sigma_\theta\right], \quad (30)$$

$$\epsilon_\theta^p = \frac{\epsilon_{EQ}}{\sigma_Y}\left[\sigma_\theta - \frac{1}{2}\sigma_r\right], \quad (31)$$

$$\epsilon_z^p = -(\epsilon_r^p + \epsilon_\theta^p), \quad (32)$$

where σ_Y is the yield stress defined earlier by Eq. (24) and ϵ_{EQ} is the equivalent plastic strain. Here, it should be noted that the above expressions for the plastic strains are exact for proportional loading, i.e. when the ratios of deviatoric stress components are held constant. However, several authors (Jahed *et al.*, 1998; Chen, 1973) pointed out the applicability of total deformation theory, and Budiansky (1959) showed that total deformation theory of plasticity may be used for a range of loading paths other than proportional loading without violating the general requirements for physical soundness of a plasticity theory.

Furthermore, using Swift's expression for nonlinear isotropic strain hardening, the relation between the yield stress σ_Y and the equivalent plastic strain ϵ_{EQ} can be expressed as

$$\sigma_Y = \sigma_0(1 + \eta\epsilon_{EQ})^{1/m}, \quad (33)$$

where η is the hardening parameter and m the material parameter. The inverse relation is

$$\epsilon_{EQ} = \left[\left(\frac{\sigma_Y}{\sigma_0}\right)^m - 1\right]\frac{1}{\eta}. \quad (34)$$

A polynomial relationship in expressing the yield stress-equivalent plastic strain relation instead of Eq. (33) is also possible (You *et al.*, 1997) and can easily be incorporated in the present model. However, Swift's hardening law will be retained here for its convenience.

Using Eqs. (24), (34) and (31) one arrives at

$$\frac{d\epsilon_\theta^p}{dr} = \frac{\sigma_Y(\sigma_r' - 2\sigma_\theta') - \sigma_Y'(\sigma_r - 2\sigma_\theta)}{2\eta\sigma_Y^2} - \frac{1}{2\eta\sigma_Y^2}\left(\frac{\sigma_Y}{\sigma_0}\right)^m\left[(m-1)\sigma_Y'(\sigma_r - 2\sigma_\theta) + \sigma_Y(\sigma_r' - 2\sigma_\theta')\right], \quad (35)$$

in which the derivative σ_Y' may conveniently be expressed as

$$\sigma_Y' = \frac{\sigma_r}{\sigma_Y}(\sigma_r' - \frac{1}{2}\sigma_\theta') + \frac{\sigma_\theta}{\sigma_Y}(\sigma_\theta' - \frac{1}{2}\sigma_r'). \quad (36)$$

The governing equation (29) for the plastic region can now be rewritten in terms of Y_p and its derivatives by virtue of Eqs. (24), (34), (30), (31) and (35) and of the definitions

$$\sigma_r = \frac{Y_p}{hr} \quad \text{and} \quad \sigma_r' = -\left[\frac{1}{r} + \frac{h'}{h}\right]\frac{Y}{hr} + \frac{Y_p'}{hr}, \quad (37)$$

$$\sigma_\theta = \frac{1}{h}\frac{dY_p}{dr} \quad \text{and} \quad \sigma_\theta' = -\frac{h'Y_p'}{h^2} + \frac{Y_p''}{h}. \quad (38)$$

Hence, Eq. (29) as well as Eq. (28) can be put into the following general form:

$$\frac{d^2Y_i}{dr^2} = f_i(r, Y_i, \frac{dY_i}{dr}). \quad (39)$$

A nonlinear shooting method using Newton iterations, as described in the Appendix, is of great advantage in solving nonlinear 2-point boundary value problems of this type.

Numerical Results

For the presentation of the numerical results we use a dimensionless radial coordinate: $\overline{r} = r/b$, dimensionless disk thickness: $\overline{h} = h/h_0$, normalized strain $\overline{\epsilon}_j = \epsilon_j E/\sigma_0$ and normalized hardening parameter $H = \eta\sigma_0/E$, in addition to nondimensional variables ($\overline{\sigma}_j$, $\overline{u}$, $\overline{p}$) defined earlier with reference to Figure 3. All the computations refer to the parabolic profile described by Eq. (1). The initiation of yielding and the propagation of the 2 plastic regions for 3 different annular disk profiles $n = 0.3$, $k = 1.02$; $n = 0.4$, $k = 1.02467$ (the critical profile) and $n = 0.4$, $k = 1.5$ are shown in Figures. 4(a), (b) and (c), respectively, as a function of dimensionless external pressure $\overline{p}$. The parameters chosen for the material hardening model are $H = 0.25$ and $m = 0.75$. As seen in Figure 4(a), for the profile with $n = 0.3$, $k = 1.02$, the yielding first starts at the outer surface at $\overline{p}_1 = 1.12382$ and later at the inner surface at $\overline{p}_2 = 1.31359$. Under the pressure $\overline{p} > \overline{p}_2$, 3 adjacent ring shaped zones are formed inside the disk, i.e. an inner plastic region, an annular elastic region and an outer plastic region. Both plastic regions expand with increasing pressures, and at $\overline{p} = \overline{p}_3 = 2.06697$, the disk becomes fully plastic when the 2 plastic regions merge at the radial location $\overline{r} = 0.46788$. In addition, for this case, the outer plastic region expands more rapidly than the inner one. Comparing the elastic-plastic response of the 3 disk profiles (Figures 4(a), (b), and (c)), it can be observed that the fully plastic pressure $\overline{p}_3$ decreased significantly ($\overline{p}_3 = 2.06697$, $\overline{p}_3 = 1.75969$, and $\overline{p}_3 = 1.57182$ for Figures 4(a), (b), and (c), respectively) as the outer edge thickness of the disk increased ($\overline{h}(1) = 0.235$, $\overline{h}(1) = 0.292$, and $\overline{h}(1) = 0.396$ for Figures. 4(a), (b), and (c), respectively).

Under the external pressure $\overline{p} = 1.7$, for the material parameters $H = 0.25$ and $m = 0.75$, the disk is in a partially plastic state with $\overline{r}_1 = 0.336$ and $\overline{r}_2 = 0.640$. The corresponding stress and plastic strain distributions are given in Figure 5(a).

The residual stresses occurring in the variable thickness annular disks upon removal of the external pressure are also determined. As long as secondary plastic flow does not occur, the residual stresses can be obtained by subtracting the stresses corresponding to unrestricted elastic behavior at the same load from those of the elastic-plastic state. The possibility of occurrence of secondary plastic flow is investigated by the determination of the values of $\overline{\sigma}_Y^R$ at the residual stress state which is defined according to the von Mises' yield criterion as

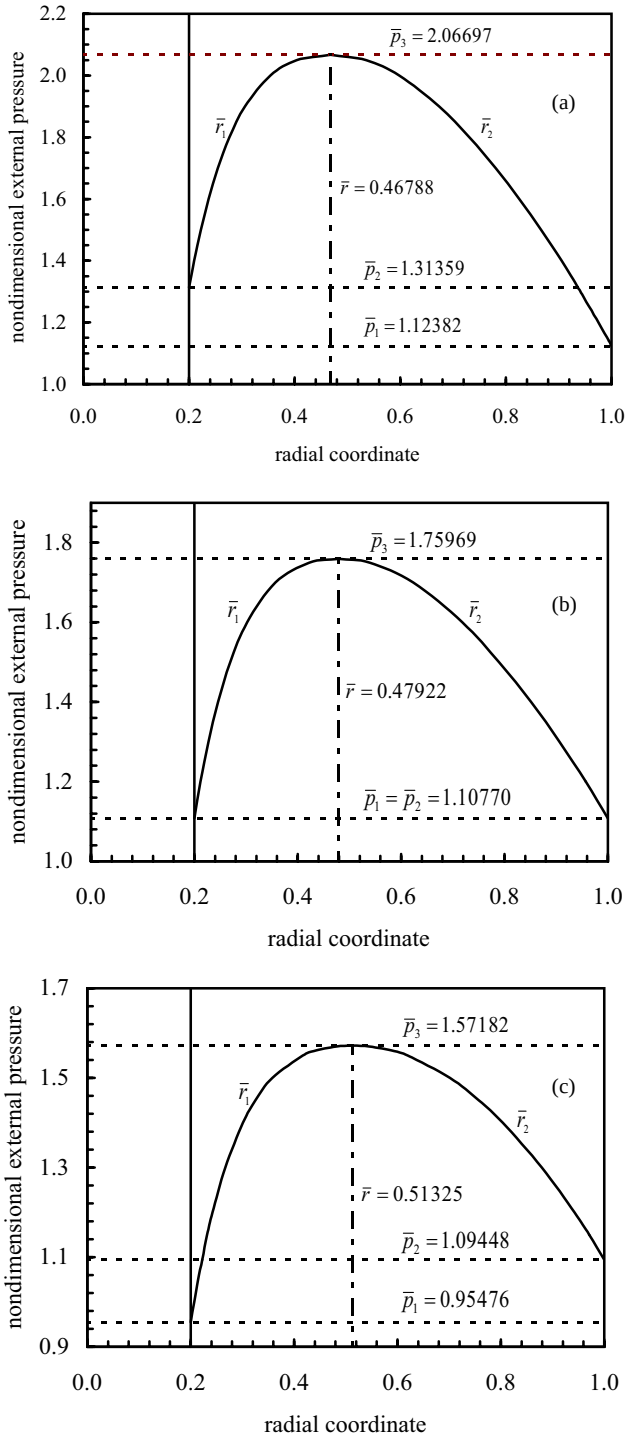

Figure 4. Expansion of plastic regions as a function of nondimensional pressure for (a) $n = 0.3$, $k = 1.02$, (b) $n = 0.4$, $k = 1.02467$, (c) $n = 0.4$, $k = 1.5$.

$$\overline{\sigma}_Y^R = \sqrt{(\overline{\sigma}_r^R)^2 - \overline{\sigma}_r^R \overline{\sigma}_\theta^R + (\overline{\sigma}_\theta^R)^2}\ . \qquad (40)$$

The residual stresses and the function $\overline{\sigma}_Y^R(\sigma_r^R, \sigma_\theta^R)$ upon removal of the pressure $\overline{p} = 1.7$ are plotted in Figure 5(b) for $m = 0.75$ (solid lines) and for $m = 1.25$ (dashed lines).

Figure 6(a) shows the stress and plastic strain distributions under the fully plastic pressure $\overline{p}_3 = 1.79954$ for $m = 0.75$. The residual stress distributions corresponding to this pressure are also shown in Figure 6(b) for $m = 0.75$ (solid lines) and for $m = 1.25$ (dashed lines; $\overline{p}_3 = 1.75968$). It can be observed in this figure that although moderately large tensile circumferential stress occurs at the inner surface, since $\overline{\sigma}_Y^R < 1$ it does not lead to secondary plastic deformation.

Concluding Remarks

The present work deals with the elastic, partially plastic and fully plastic stress and deformation response of nonuniform annular disks with nonlinear hardening material behavior under the application of external pressure. The problems of linearly hardening annular disks subject to external pressure have been treated analytically using Tresca's yield condition for hyperbolic, exponential and other forms of thickness variations in the references (Güven, 1992, 1993, 1998). In all of these studies it was considered that yielding commences at the inner surface and the plastic region formed there expands outwards and reaches the pressure loaded outer boundary at the fully plastic state. In fact, their analysis is valid provided that $\overline{a} \geq 0.5$. However, depending on the aspect ratio, thickness variation may allow plasticization to start at the outer surface at the initial or later stages of elastic-plastic deformation (see Figure 1). The present analysis focused on this aspect of deformation by employing the von Mises yield criterion, which is known to be generally more accurate than Tresca's. With the present approach nonlinear isotropic hardening in its general form can be taken into account. An efficient computational procedure using the shooting method with Newton iterations is utilized for a unified treatment of the problem under consideration.

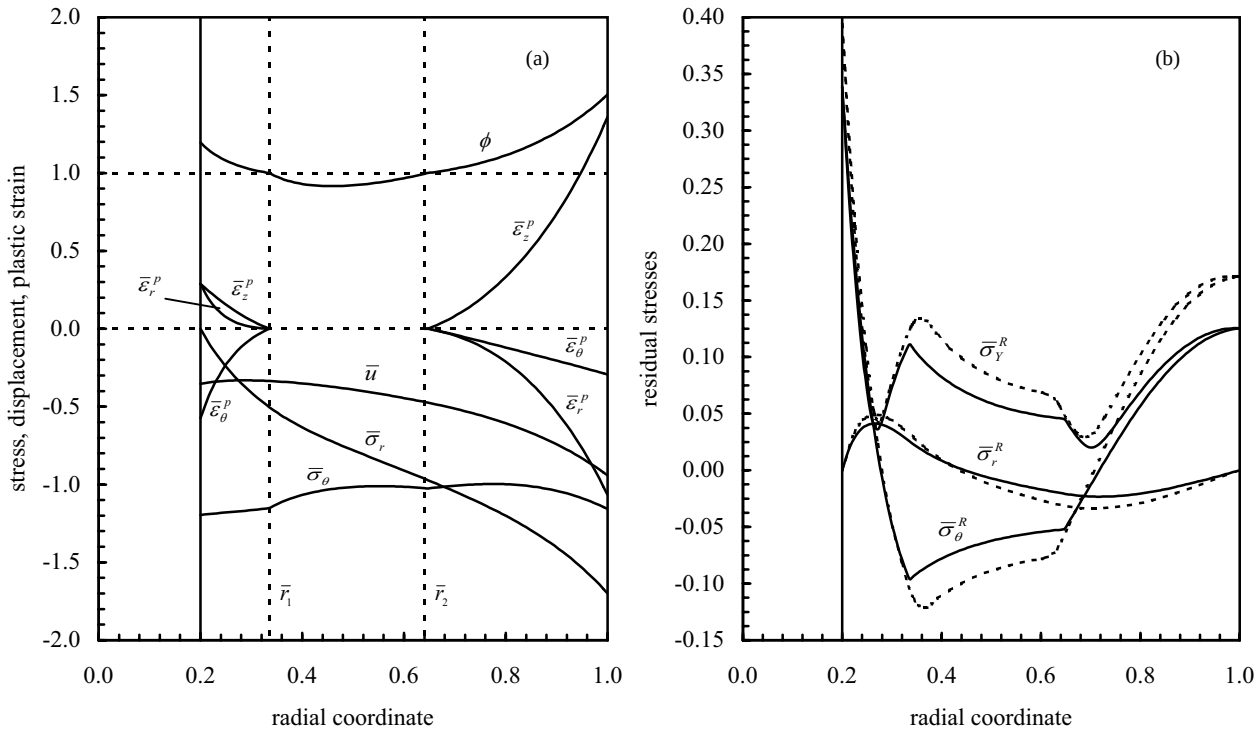

Figure 5. (a) Stresses, displacement, and plastic strains in the critical disk profile at partially plastic stress state subjected to $\overline{p} = 1.7$ for $m = 0.75$, (b) residual stresses upon removal of $\overline{p} = 1.7$ for $m = 0.75$ (solid lines) and for $m = 1.25$ (dashed lines).

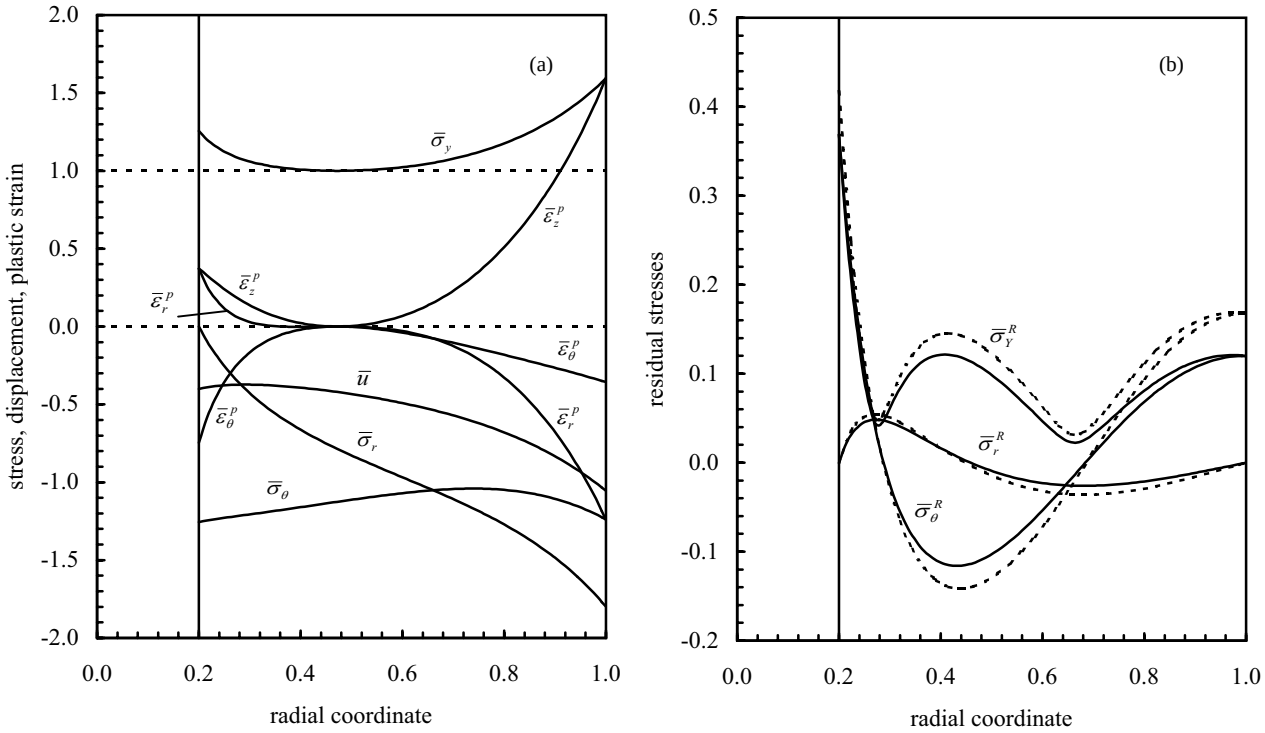

Figure 6. (a) Stresses, displacement, and plastic strains in the critical disk profile at fully plastic stress state subjected to $\overline{p} = 1.79954$ for $m = 0.75$, (b) residual stresses upon removal of $\overline{p} = 1.79954$ for $m = 0.75$ (solid lines) and for $m = 1.25$ corresponding to $\overline{p} = 1.75968$ (dashed lines).

A critical disk profile required for an optimum design for load carrying capacity is determined for which yielding sets in at the inner and outer surfaces simultaneously. The applied pressure is increased up to the values for which the intermediate elastic region vanishes. The residual stresses on removal of the external pressure are determined for various hardening and geometric parameters. It is found that unloading from any elastic-plastic state or from the fully plastic state will not lead to secondary plastic deformation. It is also observed that the pressure at which the disk becomes fully plastic is higher for the disk with the thinner outer edge.

Nomenclature

$a,\ b$	inner and outer radii of disk (dimensionless inner radius $\overline{a} = a/b$)
C_i	integration constants
E	Young's modulus
$F(\alpha, \beta, \gamma; z)$	hypergeometric function defined by Eq. (12)
$h(r)$	disk thickness function
h_0	disk thickness at the axis
m	material parameter
$n,\ k$	geometric parameters
p	external pressure (normalized form $\overline{p} = p/\sigma_0$)
r	radial coordinate (dimensionless form $\overline{r} = r/b$)
u	radial displacement (dimensionless form $\overline{u} = uE/\sigma_0 b$)
Y	stress function
γ_{ij}	shearing strain component
ϵ_{EQ}	equivalent plastic strain component
ϵ_i	elastic strain component (normalized form $\overline{\epsilon}_i = \epsilon E/\sigma_0$)
ϵ_i^p	plastic strain component
η	hardening parameter (normalized form $H = \eta\sigma_0/E$)
ν	Poisson's ratio
σ_i	stress component (dimensionless form $\overline{\sigma}_i = \sigma/\sigma_0$)
σ_i^R	residual stress component
$\sigma_0,\ \sigma_Y$	initial and subsequent yield stress

References

Abramowitz, M. and Stegun, A.I. (Eds.), Handbook of Mathematical Functions, US Government ed. Office, Fifth Printing, Washington D.C., 1966.

Budiansky, B., "A Reassessment of Deformation Theories of Plasticity". ASME Journal of Applied Mechanics 26, 259-264, 1959.

Chen, P.C.T., "A Comparison of Flow and Deformation Theories in a Radially Stressed Annular Plate". ASME Journal of Applied Mechanics 40, 283-287, 1973.

Chen, W.F. and Han, D.J., Plasticity for Structural Engineers, Springer, New York, 1988.

Eraslan A.N., "Elastoplastic Deformations of Rotating Parabolic Solid Disks Using Tresca's Yield Criterion". European Journal of Mechanics A/Solids 22, 861-874, 2003.

Eraslan, A.N. and Apatay, T., "On Annular Disks of Variable Thickness Subjected to External Pressure". Forschung im Ingenieurwesen 68, 133-138, 2004.

Eraslan A.N. and Kartal M.E., "A Nonlinear Shooting Method Applied to Solid Mechanics: Part 1. Numerical Solution of a Plane Stress Model". International Journal of Nonlinear Analysis and Phenomena 1, 27-40, 2004.

Gamer, U., "Ein Beitrag zur Spannungsermittlung in Querprebverbänden". Ingenieur-Archives of Mechanics 53, 209-217, 1984a.

Gamer, U., "The Elastic-Plastic Stress Distribution in the Rotating Annulus and in the Annulus under External Pressure". ZAMM. 64, T126-T128, 1984b.

Güven, U., "Elastic-Plastic Annular Disk with Variable Thickness Subjected to External Pressure". Acta Mechanica 92, 29-34, 1992.

Güven, U., "On the Stresses in an Elastic-Plastic Annular Disk of Variable Thickness under External Pressure". International Journal of Solids and Structures 30, 651-658, 1993.

Güven, U., "Stress Distribution in a Linear Hardening Annular Disk of Variable Thickness Subjected to External Pressure". International Journal of Mechanical Sciences 40, 589-601, 1998.

Jahed, H., Lambert, S.B. and Dubey, R.N., "Total Deformation Theory for Non-Proportional Loading". International Journal of Pressure Vessels and Piping 75, 633-642, 1998.

Mendelson A., Plasticity: Theory and Application. MacMillan New York, 1968.

Rice J.R., Numerical Methods, Software, and Analysis., 3rd ed. McGraw-Hill, Singapore, 1987.

Timoshenko, S. and Goodier, J.N., Theory of Elasticity, 3rd ed., McGraw-Hill, New York, 1970.

You, L.H., Long, S.Y. and Zhang, J.J., "Perturbation Solution of Rotating Solid Disks with Nonlinear Strain-Hardening". Mechanics Research Communications 24, 649-658, 1997.

You, L.H and Zhang, J.J., "Numerical Calculation of Elastic-Plastic Disks of Constant and Variable Thickness under External Pressure". Proceedings of Society for Design and Process Science, 231-235, 1998.

APPENDIX

The Nonlinear Shooting Method

Details of the method may be found in Eraslan and Kartal (2004). A summary is provided here. Consider a 2-point boundary value problem in the form

$$\frac{d^2\Psi}{dr^2} = G(r, \Psi, \frac{d\Psi}{dr}), \tag{41}$$

subject to the boundary conditions of type I

$$\Psi(a) = \gamma_1 \quad \text{and} \quad \alpha_2 \left.\frac{d\Psi}{dx}\right|_{x=b} + \beta_2 \Psi(b) = \gamma_2, \tag{42}$$

or of type II

$$\alpha_1 \left.\frac{d\Psi}{dx}\right|_{x=a} + \beta_1 \Psi(a) = \gamma_1 \quad \text{and} \quad \Psi(b) = \gamma_2, \tag{43}$$

where α_i, β_i and γ_i are constants.

Letting $\phi_1 = \Psi$ and $\phi_2 = \Psi'$, Eq. (41) is converted into a system of initial value problems (IVP)

$$\frac{d\phi_1}{dr} = \phi_2, \tag{44}$$

$$\frac{d\phi_2}{dr} = G(r, \phi_1, \phi_2), \tag{45}$$

subject to the initial conditions

$$\phi_1^0 = \Psi(r = a) \quad \text{and} \quad \phi_2^0 = \Psi'(r = a). \tag{46}$$

Depending on the boundary conditions (42) or (43), either one of ϕ_1^0 or ϕ_2^0 or both may be unknowns. These unknowns are computed iteratively by the application of the Newton method.

In the case of BC type I, $\phi_1(a) = \gamma_1$, that is, ϕ_1^0 is known but ϕ_2^0 is not, Newton iterations begin with an initial estimate ϕ_2^0 and at the i-th iteration cycle, the IVP system is solved 3 times with

I.	$\phi_2^0 = \phi_2^i(a)$	to give	$f_1 = \alpha_2\phi_2(b) + \beta_2\phi_1(b) - \gamma_2$,
II.	$\phi_2^0 = \phi_2^i(a) + \Delta\phi$	to give	$f_2 = \alpha_2\phi_2(b) + \beta_2\phi_1(b) - \gamma_2$,
III.	$\phi_2^0 = \phi_2^i(a) - \Delta\phi$	to give	$f_3 = \alpha_2\phi_2(b) + \beta_2\phi_1(b) - \gamma_2$,

in which $\Delta\phi$ is a small increment. Two of these solutions involving $\phi_2^i(a) \pm \Delta\phi$ are performed for the purpose of generating tangents numerically. Via central differences this tangent is $(f_2 - f_3)/2\Delta\phi$ and hence a better approximation for $\phi_2^0 = \phi_2(a)$ can now be obtained from

$$\phi_2^0 = \phi_2^{i+1}(a) = \phi_2^i(a) - \frac{(2\Delta\phi)f_1}{f_2 - f_3}. \tag{47}$$

Iterations are repeated until $\left|\phi_2^{i+1}(a) - \phi_2^i(a)\right| < \varepsilon_T$, where ε_T represents the specified error tolerance.

On the other hand, in the case of boundary conditions defined by Eq. (43), both initial conditions ϕ_1^0 and ϕ_2^0 are unknowns. In this case, ϕ_1^0 is estimated and ϕ_2^0 is calculated from $\phi_2^0 = (\gamma_1 - \beta_1\phi_1^0)/\alpha_1$ and again at the i-th iteration cycle the IVP system is solved 3 times with

I.	$\phi_1^0 = \phi_1^i(a)$	and	$\phi_2^0 = (\gamma_1 - \beta_1\phi_1^0)/\alpha_1$	to give	$f_1 = \phi_1(b) - \gamma_2$,
II.	$\phi_1^0 = \phi_1^i(a) + \Delta\phi$	and	$\phi_2^0 = (\gamma_1 - \beta_1\phi_1^0)/\alpha_1$	to give	$f_2 = \phi_1(b) - \gamma_2$,
III.	$\phi_1^0 = \phi_1^i(a) - \Delta\phi$	and	$\phi_2^0 = (\gamma_1 - \beta_1\phi_1^0)/\alpha_1$	to give	$f_3 = \phi_1(b) - \gamma_2$.

A Newton iteration equation similar to Eq. (47) is then used to successively correct ϕ_1^0.

The initial value system defined by Eqs. (44) and (45) is solved numerically by the use of the Runge-Kutta Fehlberg predictor corrector method (Rice, 1987). The main advantages of this procedure are accuracy provided by higher order Runge Kutta methods and rate of convergence. Only a few iterations are performed to arrive at convergence and this rate depends weakly on the initial estimates to start the computations.